Journal of Cellular Biochemistry 98:861–871 (2006)

Overexpression of Caveolin-1 Results in Increased Plasma Membrane Targeting of Glycolytic Enzymes: The Structural Basis for a Membrane Associated Metabolic Compartment

Leena S. Raikar, Johana Vallejo, Pamela G. Lloyd, and Christopher D. Hardin*

Department of Medical Pharmacology and Physiology, University of Missouri, Columbia, Missouri 65212

Abstract Although membrane-associated glycolysis has been observed in a variety of cell types, the mechanism of localization of glycolytic enzymes to the plasma membrane is not known. We hypothesized that caveolin-1 (CAV-1) serves as a scaffolding protein for glycolytic enzymes and may play a role in the organization of cell metabolism. To test this hypothesis, we over-expressed CAV-1 in cultured A7r5 (rat aorta vascular smooth muscle; VSM) cells. Confocal immunofluorescence microscopy was used to study the distribution of phosphofructokinase (PFK) and CAV-1 in the transfected cells. Areas of interest (AOI) were analyzed in a central Z-plane across the cell transversing the perinuclear region. To quantify any shift in PFK localization resulting from CAV-1 over-expression, we calculated a periphery to center (PC) index by taking the average of the two outer AOIs from each membrane region and dividing by the central one or two AOIs. We found the PC index to be 1.92 ± 0.57 (mean $\pm$ SEM, $N = 8$) for transfected cells and 0.59 ± 0.05 (mean $\pm$ SEM, $N = 11$) for control cells. Colocalization analysis demonstrated that the percentage of PFK associated with CAV-1 increased in transfected cells compared to control cells. The localization of aldolase (ALD) was also shifted towards the plasma membrane (and colocalized with PFK) in CAV-1 over-expressing cells. These results demonstrate that CAV-1 creates binding sites for PFK and ALD that may be of higher affinity than those binding sites localized in the cytoplasm. We conclude that CAV-1 functions as a scaffolding protein for PFK, ALD and perhaps other glycolytic enzymes, either through direct interaction or accessory proteins, thus contributing to compartmented metabolism in vascular smooth muscle. J. Cell. Biochem. 98: 861–871, 2006.

Key words: caveolae; glycolysis; phosphofructokinase; scaffolding protein; smooth muscle

Glycolysis is a ubiquitous metabolic pathway in mammals and has traditionally been viewed as a pathway consisting of enzymes freely diffusing throughout the cytoplasm. However, over the last few decades increasing evidence has suggested that glycolytic enzymes are localized to a number of different elements of the cytoarchitecture (e.g.,: [Jenkins et al., 1984; Knull et al., 1987; Pagliaro and Taylor, 1988, 1992; Beitner, 1993; Ouporov et al., 1999]), and that pathway fluxes may be compartmented or channeled [Lynch and Paul, 1983; Clegg and Jackson, 1989; Hardin and Kushmerick, 1994; Hardin and Roberts, 1995a; Goodwin et al., 1996; Hardin and Finder, 1998]. Glycolytic enzyme associations with elements of the cytoskeleton (actin filaments and microtubules) as well as cellular membranes have been reported. While the specific binding motifs for glycolytic enzyme associations have been reported for associations with actin [Ouporov et al., 1999, 2000] and microtubules [Lehotzky et al., 1993; Volker and Knull, 1993; Volker et al., 1995; Vertessy et al., 1996; Lloyd and Hardin, 1999], the only specific mechanism

Abbreviations used: AOI, area of interest; CAV-1, caveolin-1; PC index, peripheral to central index; PFK, phosphofructokinase; VSM, vascular smooth muscle; ALD, aldolase.

Grant sponsor: NIH (to CDH); Grant number: DK60668; Grant sponsor: Porter Fellowship from the American Physiological Society (JV).

*Correspondence to: Christopher D. Hardin, PhD, Department of Medical Pharmacology and Physiology, MA 415 Medical Sciences Building, University of Missouri, Columbia, MO 65212. E-mail: HardinC@missouri.edu

Received 16 May 2005; Accepted 28 October 2005

DOI 10.1002/jcb.20732

for membrane association of glycolytic enzymes has been reported in erythrocytes, where they are associated with the transmembrane protein band 3 anion transporter [Jenkins et al., 1985; Low et al., 1993; von Ruckmann and Schubert, 2002; Campanella et al., 2005]. Therefore, the mechanisms by which glycolytic enzymes associate with cellular membranes are poorly understood.

Smooth muscle has been a useful model system for studying the organization of glycolysis. Early work showed that smooth muscle had a very high rate of glucose conversion to lactate even under well oxygenated conditions (see [Paul, 1980]) and that as much as 30% of the cellular ATP production was derived from glucose conversion to lactate [Hardin and Paul, 1995]. Work using radioisotopes [Lynch and Paul, 1983] and stable isotope tracers [Hardin and Kushmerick, 1994; Hardin and Roberts, 1995a; Hardin and Finder, 1998] has provided evidence for a compartmentation of pathways of carbohydrate metabolism including glycolysis, and gluconeogenesis. Channeling of intermediates has also been reported in permeabilized smooth muscle cells [Hardin and Finder, 1998]. The function of localized glycolysis in smooth muscle has been proposed to be to provide specifically localized energetic support to ATP demanding functions such as the Na^+-pump [Lynch and Paul, 1987; Campbell and Paul, 1992], the Ca^{2+}-pump [Paul et al., 1989; Hardin et al., 1992], and Rho-kinase signaling [Leach et al., 2001].

We (and others) have recently reported the association of glycolytic enzymes with the caveolin family of membrane proteins. Caveolins are primarily responsible for the formation of small invaginations of 60–100 nm diameter in the plasma membrane that have been proposed to provide binding or targeting site for various signal transduction and lipid transport proteins [Anderson, 1998; Luetterforst et al., 1999; Machleidt et al., 2000; Thyberg, 2000; Razani et al., 2002]. Caveolae represent a subdomain of the plasma membrane, which is enriched in cholesterol and glycosphingolipids [Anderson, 1998; Smart et al., 1999]. CAV-1 and -2 are expressed in endothelial cells, fibroblasts and adipocytes, while caveolin-3 is expressed only in muscle cells [Schlegel and Lisanti, 2001; Razani et al., 2002]. To date, the expression of all three caveolin isoforms has been reported only in smooth muscle cells, with localization predominantly at the plasma membrane in freshly isolated smooth muscle cells [Taggart, 2001]. Recent studies report that in differentiated skeletal C2C12 myotubes, PFK associates with caveolin-3 [Scherer and Lisanti, 1997; Sotgia et al., 2003]. We have shown that CAV-1 recruits PFK to the plasma membrane region in smooth muscle cells [Vallejo and Hardin, 2004a], and lymphocytes [Vallejo and Hardin, 2005].

The association of PFK with CAV-1 has been demonstrated in limited instances such as in cells (Cos-7 and lymphocytes) that do not normally express caveolin. Since glycolytic enzymes bind to a number of structures in the cytoplasm, it was of interest to determine whether provision of additional CAV-1 protein would increase the amount of CAV-1 in the plasma membrane, and whether the overexpressed CAV-1 could redirect PFK and other glycolytic enzymes to the membrane.

MATERIALS AND METHODS

Cell Culture

The A7r5 VSM cell line from rat aorta (American Type Culture Collection, Manassas, VA), was grown in 75 cm^2 flasks (Corning, Cambridge, MA) and on 25 mm-diameter glass coverslips (Fisherbrand, Pittsburgh, PA) or on four-well chambered coverglass (Nalge Nunc International, Naperville, IL) in Dulbecco's modified Eagle's medium (DMEM, Sigma, St. Louis, MO) with added 5.5 mM D-glucose, 26.2 mM Na_2HCO_3, 1 mM sodium pyruvate, and 4 mM L-glutamine. DMEM was supplemented with 10% fetal bovine serum (Gibco, Grand Island, NY) and 1% antibiotic antimycotic solution (Sigma). Cell propagation was done in a 5% CO_2/humidified chamber at 37°C and the medium was changed every other day to avoid microbial contamination.

Transfection With CAV-1 cDNA

A7r5 cells were transfected with pCI-NEO vector containing the coding sequence for human CAV-1 (generously provided by Dr. Eric Smart, University of Kentucky) using a Tfx delivery solution. Cells from 75 cm^2 flasks were used at ~80% confluency. Two sterile culture tubes were prepared. One tube contained 7.5 ml of serum free culture media with 19.95 μg of the plasmid, and the other contained only 7.5 ml of serum free culture media for mock transfection. The tubes were vortexed and 89.7 μl of Tfx

reagent (Promega, Madison, WI) was added to each tube. The tubes were vortexed again and incubated at room temperature for 10–15 min. Subsequently, the media from both flasks were discarded and the Tfx/DNA mixture was added. After 1 h of incubation at 37°C, the flasks were filled with 16.5 ml culture media containing serum and incubated for 48 h at 37°C.

Selection for Stably Expressing A7r5 Cells

The antibiotic G-418 sulfate (Promega, Madison, WI) was included in the culture media to select transfected cells. Two days after the cells were transfected, the media was changed to include G-418 sulfate at a concentration of 50 μg/100 ml. Once all the cells of the mock transfection died, the G-418 sulfate concentration was lowered to 20 μg/100 ml for longer term culture.

Cell Lysate Preparation

Cultured A7r5 cells grown previously in 75 cm^2 flasks and transfected with CAV-1 were transferred to a 15 ml Falcon tube after treatment with Trypsin-EDTA (Sigma) and centrifuged at 2,600*g* and 25°C for 5 min. Pelleted cells were resuspended in 200 μl of ice-cold lysis buffer [3.51 g octyl glucopyranoside, 2.0 ml Triton X-100, 1.75 g NaCl, 0.97 g 2N-Morpholino ethanesulfonic acid (pH 6.4)], transferred to a 1.5 ml centrifuge tube and incubated at 30 min at 4°C. Then the cell lysate was sonicated (ELMA sonciator Transsonic Digital Sonicator) for 10 min at maximum power. Finally, the lysate was centrifuged at 1,5000*g* and 4°C for 10 min. The supernatant fraction was transferred to a fresh centrifuge tube and stored at −20°C until SDS–PAGE and Western Blot analysis was performed.

SDS–PAGE and Western Blot Analysis

A7r5 cell lysates were separated by SDS–PAGE using a 4%–12% Bis-Tris Criterion XT precast gel (Bio-Rad, Hercules, CA) and then electrotransferred to a 0.2 μm Immuno-Blot PVDF membrane (BioRad, Hercules, CA) sheet for Western blot analysis. The protein concentration of each concentration was determined by a Bradford Assay (Bio-Rad). After being transferred, the PDVF membrane sheets were immunolabeled with rabbit polyclonal CAV-1 pAb (1:2,000) (BD Transduction Laboratories, Lexington, KY) followed by alkaline phosphatase-conjugated donkey anti-rabbit IgG (1:1,000) (Rockland Immunochemicals for Research, Gilbertsville, PA). The PDVF membrane was developed in alkaline phosphatase developing buffer (Bio-Rad) to visualize protein bands. Quantification of the intensity from protein bands was performed by analysis using UN-SCAN-IT gel version 4.3 (Silk Scientific, Orem, UT) software after creating a digital scan of the membrane using FluorChem 8800 (Alpha Innotech, San Leandro, CA). AOI's were created and the total intensity of the pixels within each protein band was determined using the software. The background intensity of the membrane was subtracted from the value of each AOI to standardize measurements between the different lanes. Finally, intensity values from different protein bands were analyzed to determine the percentage difference in intensity.

Immunofluorescence Labeling

The transfected cells were fixed in suspension with a paraformaldehyde solution (2% paraformaldehyde, 350 NaCl, 160 mM HEPES, and 10 mM $CaCl_2$). Fixed cells were then incubated in a permeabilization solution (500 μM β-escin, 150 mM NaCl, and Na-citrate) containing 1% normal donkey serum (Sigma). After the initial permeabilization, cells were incubated overnight in permeabilization solution with 1% normal donkey serum, goat anti-rabbit PFK IgG (1:100) (Rockland Immunochemicals for Research, Gilbertsville, PA), and either mouse monoclonal anti-CAV-1 IgG (1:100) (Research Diagnostics, Inc., Flanders, NJ) or sheep anti-rabbit aldolase PAb (1:100) (Nordic Immunological Laboratories, Tilburg, Netherlands). After incubation with both primary antibodies, cells were incubated for 3 h in permeabilization solution containing 1% BSA, donkey anti-goat IgG conjugated to Alexa 488 (green) (1:100) (Molecular Probes, Eugene, OR) and donkey anti-mouse IgG conjugated to Alexa 568 (for ALD detection) or 594 (for PFK detection) (red) (1:100) (Molecular Probes). Subsequently, cells were rinsed with a solution containing 150 mM NaCl, 15 mM Na-citrate, and 2% BSA. Finally, cells were transferred to glass slides and glass chambers containing Mowiol 4-88 mounting medium.

Confocal Microscopy and Image Analysis

Laser scanning confocal microscopy was performed using the BioRad Radiance 2000 (BioRad, Hercules, CA) on an Olympus IX-70

inverted microscope (Olympus, Tokyo, Japan). Images were captured using a 60X water immersion objective (1.2 UPlan Apo) with a confocal pinhole size of 1.2 μm and transmitted to a personal computer with the software programs BioRad LaserSharp 2000 (BioRad) and MetaMorph™ 4.6.9 (Universal Imaging, Chesterfield, PA). All fluorescence images were acquired using the excitation lasers (BioRad) ArKr/Ar 488 (for green) and Kr/Ar 568 (for red) and emission filters (BioRad) of 515 ± 30 nm (for green) and 600 ± 40 nm (for red). All transmitted light images were acquired with Nomarski optics using a 637 nm red diode laser. Image acquisition was done in the X, Y, and Z dimensions with X-Y resolution of 0.09 μm, Z-steps of 0.75 μm and a final image size of 1,024 × 1,024 pixels for all images. The magnification (zoom = 2), laser iris (iris = 1.9 μm), gain, and offset parameters were optimized for each laser (ArKr/Ar 488, Kr/Ar 568, and 637 nm red diode laser) and were kept constant for all images. MetaMorph™ 4.6.9 software was used for imaging processing after acquisition. For each image, the central Z-plane was carefully selected. The ratio of overlapping signals from the green-fluorescence and red-fluorescence images from each sample was reviewed by creating an overlay image. Finally, an analysis of PFK distribution across the cell was performed using the central Z-plane from each A7r5 sample. Identical AOIs (30 pixels^2) were created strictly aligned across the entire axis of each cell crossing immediately adjacent to the nuclear membrane while avoiding pixels inside the nuclei. Each individual AOI was analyzed using MetaMorph to display the dimensional and pixel intensity statistics of the selected region of interest. The average pixel intensity within each AOI was determined and plotted as a function of percentage distance across cell.

Determination of the Relative Peripheral and Central Localization of PFK

Areas of interest (AOI) were sampled across the span of the cell near the perinuclear region. AOIs in the periphery (the two AOIs nearest each of the plasma membrane edges) and in the center (the center of the cell in the perinuclear region) were used. Signal intensity was measured in each AOI and we calculated the peripheral to center ratio for PFK fluorescence (P/C ratio). The P/C ratio was the mean intensity in the peripheral AOIs divided by the mean intensity of the central AOIs. This ratio was used as an index to compare the relative distribution of PFK in the plasma membrane region compared to that in the central portion of the cytoplasm as an index of membrane localization.

Statistical Analysis

Results are expressed as the mean ± SEM of n = 8 for transfected cells and n = 11 for control cells. Statistical significance was determined using a two-tailed paired Student's *t*-test assuming unequal variances. *P*-value ≤ 0.05 were considered significant. All statistical calculations were performed using Microsoft Excel 2003 software.

RESULTS

CAV-1 Transfected Cells Over-Express CAV-1

A7r5 cells transfected with the CAV-1 containing plasmid expressed significantly more CAV-1 than non-transfected (control) cells. Shown in Figure 1 is a Western blot for CAV-1

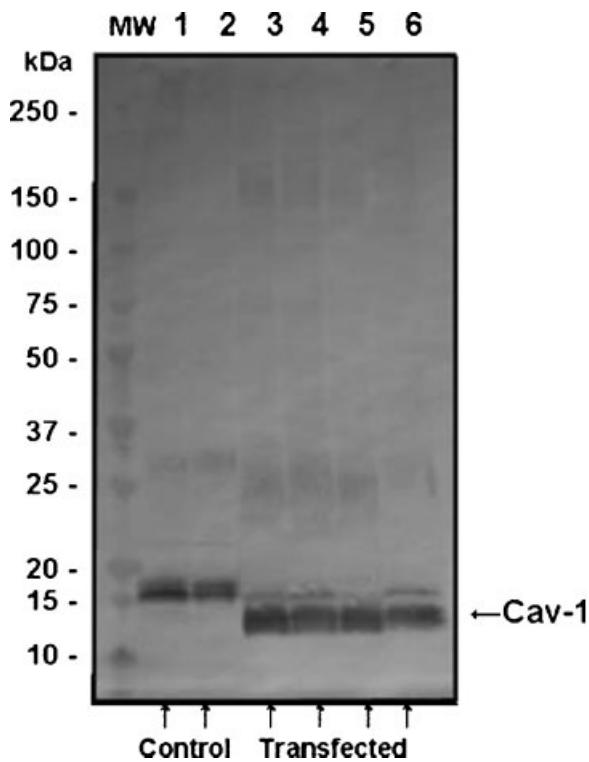

Fig. 1. Western blot analysis demonstrates the over-expression of CAV-1 in transfected cells (**Lanes 3–6**) compared to the control Cells (**Lanes 1–2**). The percentage of CAV-1 in over-expressing cells (146268.25 ± 10288.53 pixel intensity, mean ± SEM, n = 4) was significantly higher ($P < 0.05$) than control cells (95,640 ± 7,675 pixels intensity SEM, n = 2).

protein. The lanes for transfected cells show an apparent decrease in the size of the CAV-1 expressed cells compared to control cells. However, a narrow band corresponding to the wild-type also appears in the transfected cell columns. These data indicate a significant over-expression of CAV-1 in transfected cells with the plasmid encoded CAV-1 having a smaller apparent size. Treatment with deglycosylating enzymes (for both N and O-linked glycosylation) did not alter the apparent size of any of the CAV-1 bands (data not shown). Therefore, the differences in apparent size do not appear to be due to differences in the extent of glycosylation.

CAV-1 and PFK (Co)localization in Cultured A7r5 VSM Cells

In A7r5 cells, both CAV-1 and PFK exhibit abundant immunofluorescence as shown in Figure 2. Although CAV-1 is largely localized to the plasma membrane in freshly isolated and fully differentiated cells, in cultured A7r5 cells there is a distribution of both CAV-1 and PFK that is rather diffuse throughout the cell. Figure 2 shows examples of central Z-planes of images of three cells with filters for measurement of Alexa 488 (green, left column for PFK) and Alexa 594 (red, center column for CAV-1). Despite the diffuse localization of both PFK and

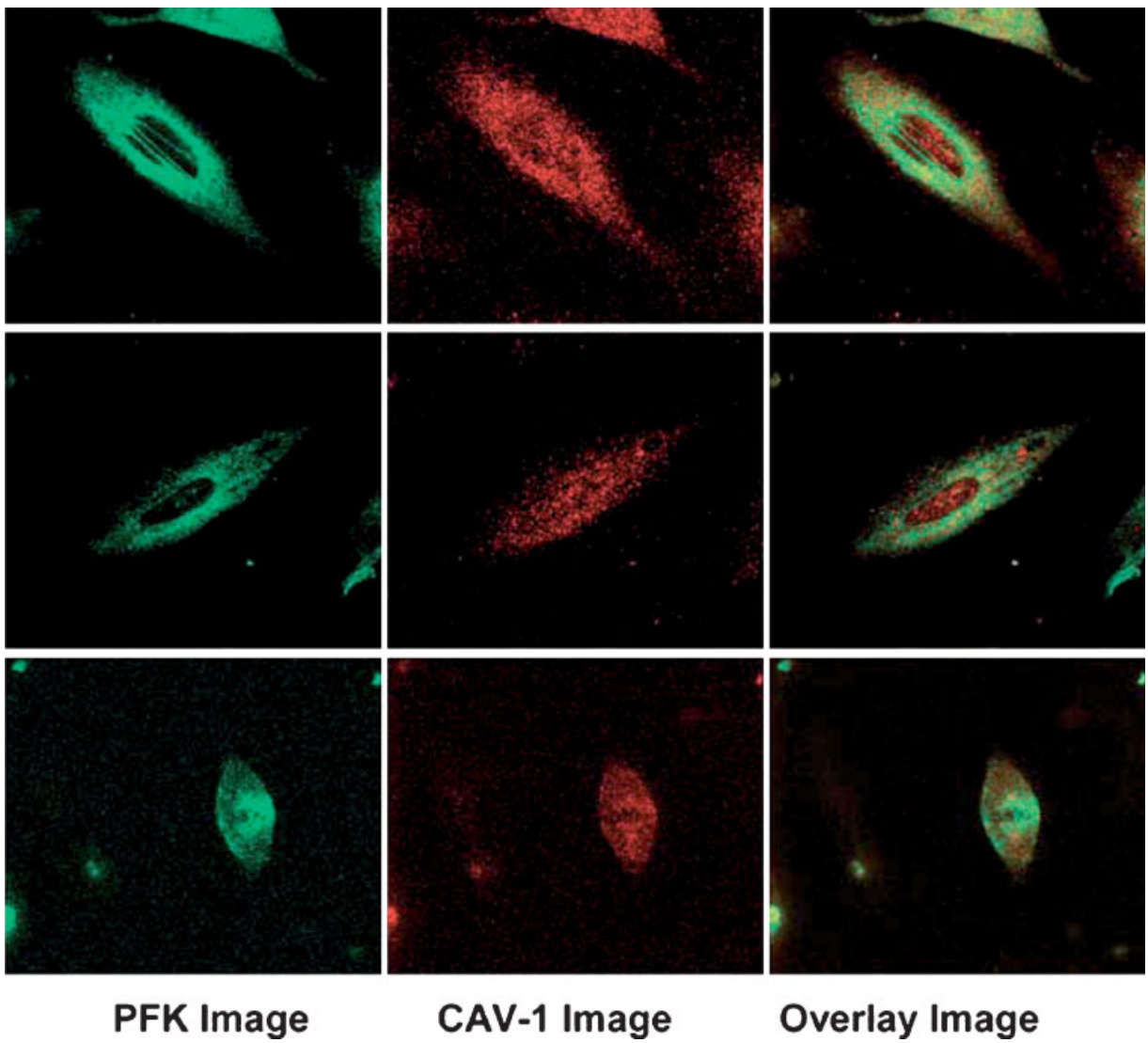

Fig. 2. Confocal immunofluorescence images of three control cultured A7r5 VSM cells immunolabeled for PFK (green, **left panels**) and CAV-1 (red, **middle panels**). The overlap of CAV-1 and PFK is shown as yellow in the right column of panels.

CAV-1, there is some colocalization of PFK and CAV-1 throughout the cell (Fig. 2, yellow color in the overlap panels).

Over-Expression of CAV-1 Results in Increased Localization of CAV-1 and PFK to the Plasma Membrane Region

To determine whether the apparent colocalization of PFK and CAV-1 was due to a specific interaction between the two proteins and whether one protein could serve as scaffolding for the other, we increased expression of CAV-1 in A7r5 cells. We predicted that if CAV-1 acted as a binding site or a scaffold protein for PFK localization, then an increase in expression and targeting of CAV-1 would alter the distribution of PFK in the cell with the PFK distribution paralleling the CAV-1 distribution. Figure 3 shows representative confocal immunofluorescence images of three cells that were transfected with a CAV-1 containing plasmid and over-expressed CAV-1. Compared to Figure 2, visual inspection of Figure 3 demonstrates increased signal from both CAV-1 and PFK in the cell periphery near the plasma membrane representing a net shift in CAV-1 and PFK away from the center of the cell and towards the periphery. The over-expressed CAV-1 was clearly targeted to the plasma membrane area and PFK localization appeared to follow CAV-1 localization.

To quantify the alteration in distribution of CAV-1 and PFK in CAV-1 over-expressing cells compared to control cells, we examined the PFK signal intensity profile across the cell in the

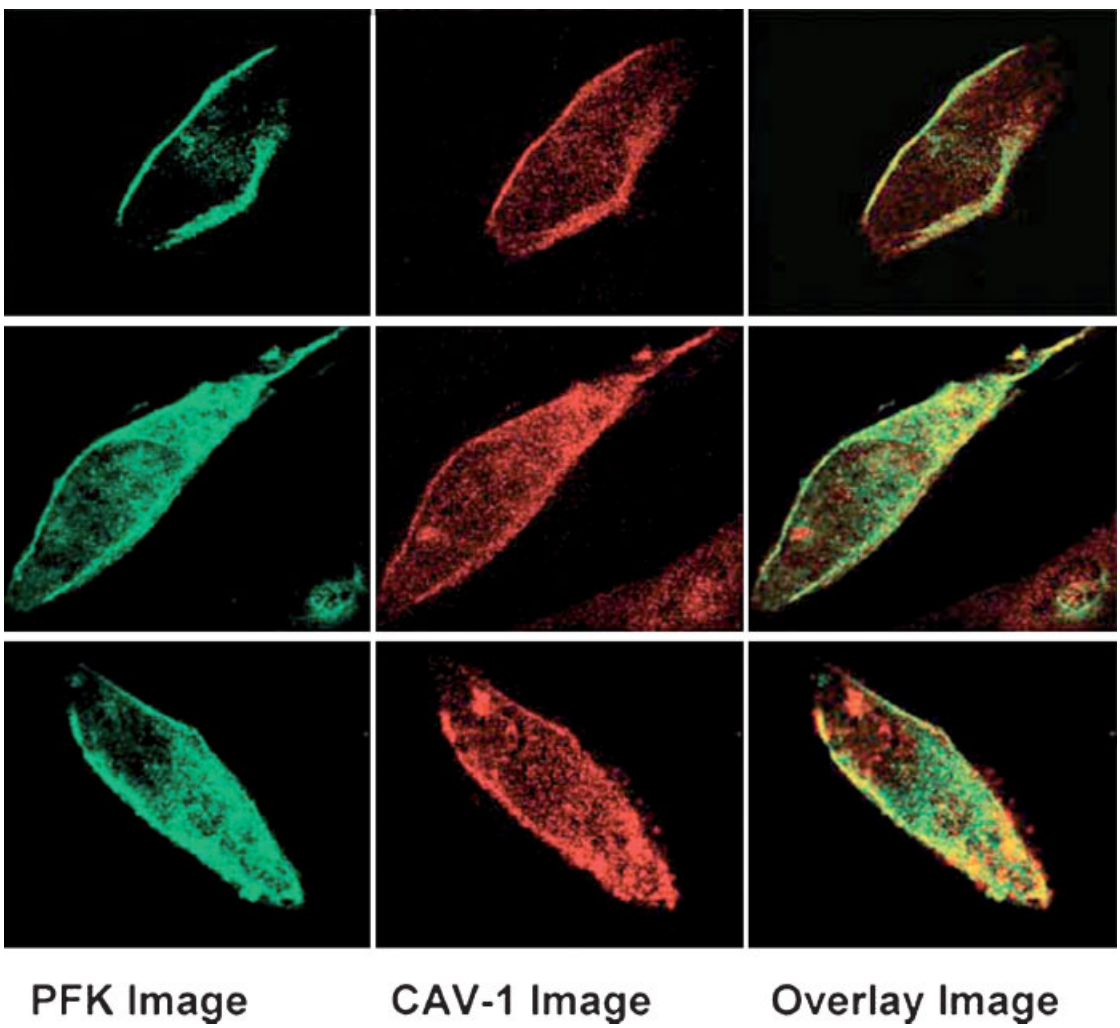

Fig. 3. Confocal immunofluorescence images of three cultured A7r5 VSM cells stably over-expressing CAV-1 and immunolabeled for PFK (green, **left panels**) and CAV-1 (red, **middle panels**). The overlap of CAV-1 and PFK is shown as yellow in the right column of panels.

middle Z-stage image. Areas of interest (AOI) were chosen to span linearly from one plasma membrane edge across the perinuclear region, and back to the opposite plasma membrane edge (see Fig. 5A). The PFK signal intensity in the AOI plotted versus distance across the cell is shown in Figure 4 for control cells (Fig. 4A) and for CAV-1 over-expressing cells (Fig. 4B). Each cell distribution is depicted as an individual line in Figure 4. There is an apparent shift in the PFK profile towards the cell periphery in CAV-1 over-expressing cells, compared to control cells.

We calculated the periphery to center ratio of the signal intensity by taking the average of the two most peripheral AOIs on either side of the cell (for the peripheral intensity) and dividing by the one or two most central AOIs (for the central intensity) (see Fig. 5A). Figure 4B shows the periphery to center ratio (P/C) of PFK intensity in control and CAV-1 over-expressing cells. The P/C increased more than three-fold ($P = 0.026$) in CAV-1 over-expressing cells compared to control cells. Therefore, over-expression of CAV-1 resulted in increased targeting of PFK consistent with CAV-1 acting as a binding site for PFK.

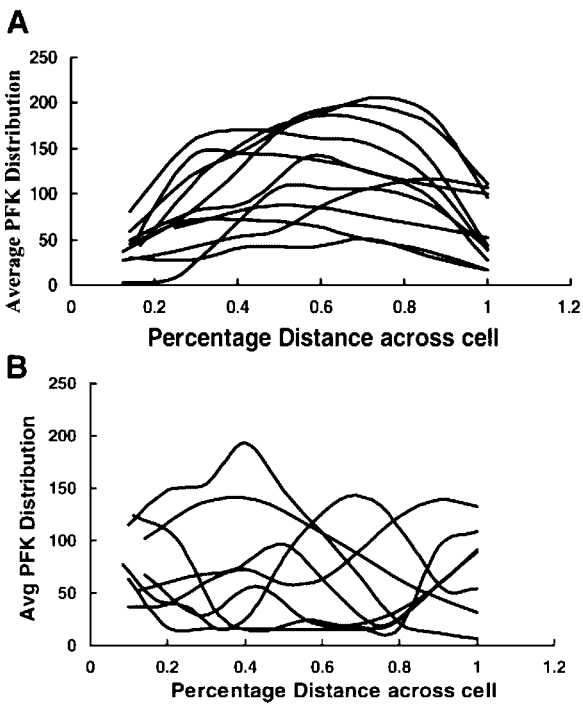

Fig. 4. Analysis of the average PFK intensity across cultured A7r5 VSM cells. **A**: control A7r5 cells, **(B)** stable CAV-1 over-expressing A7r5 cells. Analysis of PFK distribution across the cell was performed using the central Z plane from each A7r5 sample. Then identical AOIs (30 pixels^2) were created strictly aligned across the entire axis of each cell crossing right next to the nuclear membrane while avoiding pixels inside the nuclei.

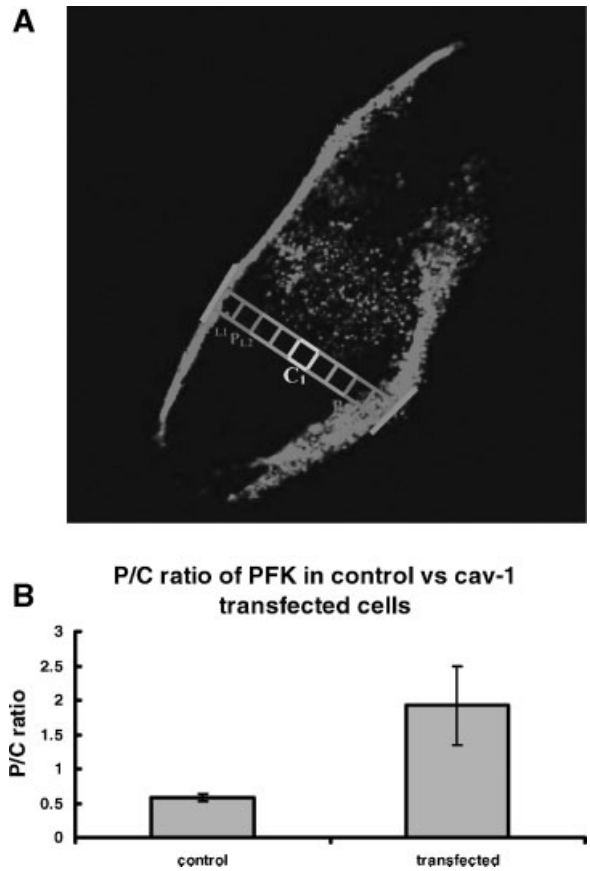

Fig. 5. **A**: AOI sampling strategy to determine the relative distribution of PFK in the cell periphery (adjacent to the plasma membrane) and the center of the cell in the perinuclear region. The peripheral to center ratio (P/C ratio) was calculated as

$$\text{PC index} = \frac{(\text{PL1} + \text{PL2} + \text{PR1} + \text{PR2})/4}{\text{C1 or } (\text{C1} + \text{C2})/2}.$$

B:The measures P/C ratio for PFK in normal (control) or stably over-expressing (transfected) A7r5 cells.

Over-Expression of CAV-1 Creates more Binding Sites for PFK and Increases PFK-CAV Interaction

Using MetaMorph software, we examined the overlap of PFK and CAV-1 in whole cell series of Z-sections. As shown in Figure 6, there is overlap of CAV-1 and PFK in control cells, despite the apparent diffuse localization of PFK and CAV-1 in these cells (see Fig. 2). However, over-expression of CAV-1 with apparent targeting to the plasma membrane area (see Fig. 3) resulted in a significant increase in the proportion of total PFK that was colocalized with CAV-1. The proportion of total CAV-1 that was colocalized with PFK also tended to increase

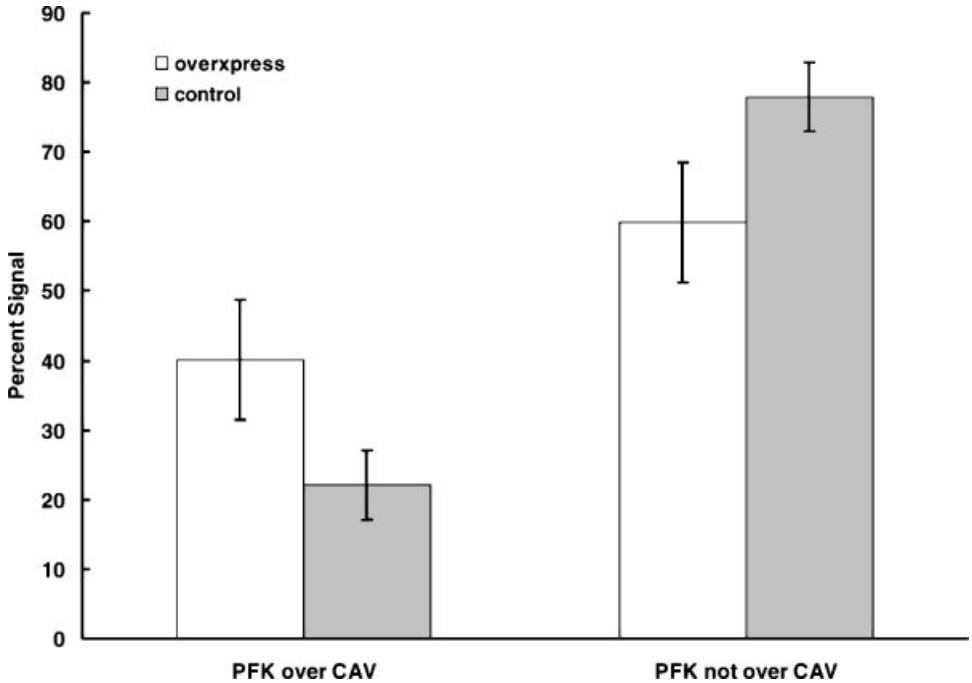

Fig. 6. Overlap of PFK with CAV-1 in cultured A7r5 cells. Specific quantification of the overlap in between PFK and CAV-1 determined by overlay of the PFK and CAV-1 images from each respective cell using MetaMorph software. Data represent the mean from seven cells for stable CAV-1 expressing cells and 10 cells for control A7r5 cells. The percentage of PFK, which overlapped with CAV-1 was significantly higher ($P < 0.05$) in stable CAV-1 over-expressing cells compared to control cells.

($P = 0.15$). Therefore, CAV-1 over-expression increases the percentage of PFK in the cell that is colocalized with CAV-1. These results are consistent with CAV-1 acting as an anchor protein for PFK in A7r5 cells.

Colocalization of Aldolase(ALD) and PFK in CAV-1 Over-Expressing Cells

To determine whether another glycolytic enzyme may also be influenced by CAV-1 over-expression, we examined the colocalization of PFK and ALD in control and CAV-1 over-expressing cells. As shown in Figure 7, CAV-1 over-expression resulted in the same redistribution of PFK to the cell periphery (membrane). In addition, ALD appeared to follow PFK (and hence CAV-1) towards the plasma membrane. Therefore, CAV-1 appears to play a role in the localization of both PFK and ALD in these VSM cells.

DISCUSSION

A necessary condition for compartmentation to occur between two pathways sharing common enzymatic steps is a spatial separation of the two pathways. Our previous work has demonstrated a compartmentation of glycolysis and gluconeogenesis in vascular smooth muscle [Hardin and Roberts, 1995a,b; Lloyd and Hardin, 1999, 2000]. Enzymes for glycolysis may exist in multiple compartments and be associated with several components of the cellular architecture such as the contractile filaments [Hardin and Paul, 1992], the microtubules [Lloyd and Hardin, 1999] and the plasma membrane [Paul et al., 1989; Hardin et al., 1992], specifically the caveolar subdomain of the plasma membrane [Lloyd and Hardin, 2001; Vallejo and Hardin, 2004b]. The gluconeogenic enzymes responsible for the conversion of exogenously applied fructose 1,6-bisphosphate to glucose have been hypothesized to be localized to the plasma membrane in non-caveolar regions [Lloyd and Hardin, 2000, 2001; Vallejo and Hardin, 2005]. Therefore, there may be multiple glycolytic compartments within the VSM cell and one or more gluconeogenic compartments.

Since there are multiple locations within the cytoplasm responsible for localizing glycolytic enzymes (and hence localizing the flux within

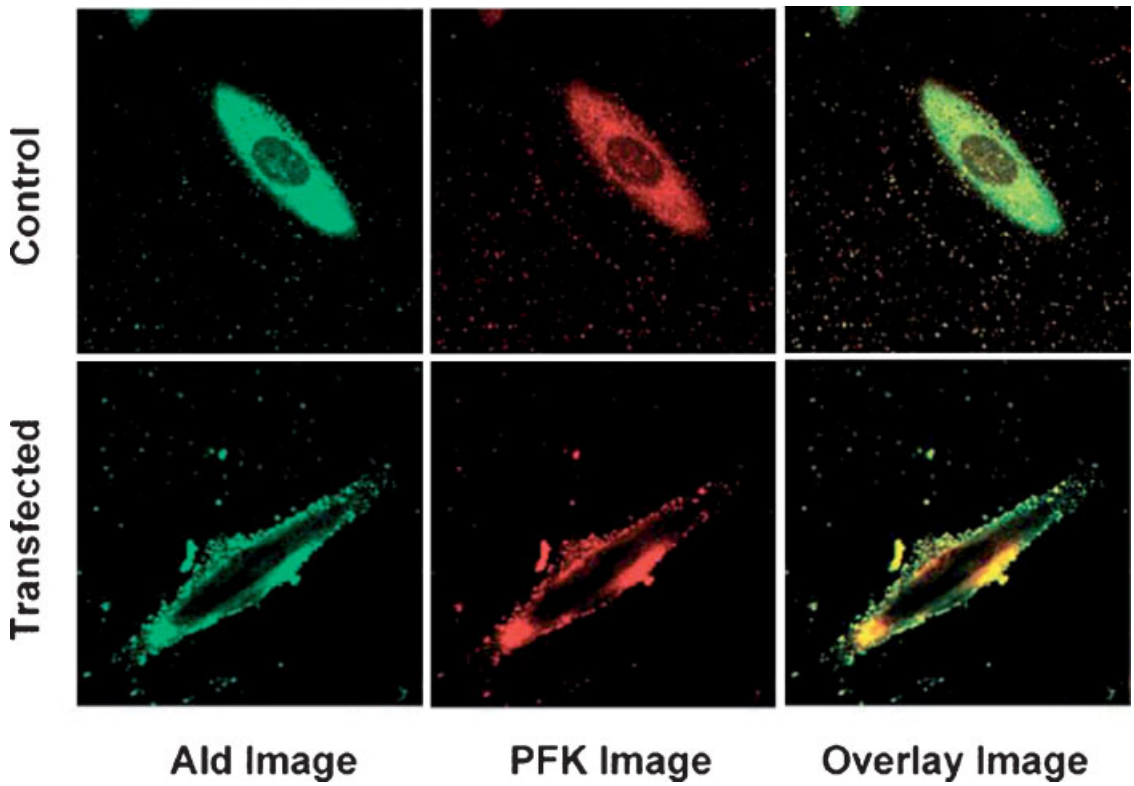

Fig. 7. Confocal immunofluorescence images of control (**top row**) and stably over-expressing CAV-1 (**bottom row**) cultured A7r5 VSM cells immunolabeled for Ald (green, **left panels**) and PFK (red, **middle panels**). The overlap of Ald and PFK is shown as yellow in the right column of panels.

each glycolytic compartment), the relative number of enzyme binding sites as well as the affinity of the binding sites should determine the distribution of glycolytic enzymes within the cytoplasm. We have previously provided evidence that CAV-1 is responsible for localizing the glycolytic enzyme PFK to the caveolar regions of the plasma membrane in smooth muscle [Vallejo and Hardin, 2004a,b] and in lymphocytes transfected with CAV-1 [Vallejo and Hardin, 2005]. Similarly, in skeletal muscle, caveolin-3 may help target PFK to the plasma membrane [Sotgia et al., 2003]. The fraction of a given glycolytic enzyme that is targeted to the caveolae should be dependent on the number of CAV-1 binding sites as well as the relative affinity of CAV-1 compared to other scaffolding proteins for PFK in the cytoplasm (tubulin, actin, etc.). Although demonstration of the possible role of CAV-1 in the localization of PFK to the plasma membrane was a key step in understanding the mechanisms of the localization of the glycolytic pathway to the plasma membrane, at least two issues remained unclear. First, does an increase in CAV-1 in a cell that normally expresses CAV-1 result in shifts in glycolytic enzyme distribution (or do other sites inside the cell retain the same amount of bound enzyme)? Second, does CAV-1 contribute to the localization of only PFK or can it also localize other glycolytic enzymes to the plasma membrane?

When A7r5 cells were over-expressed with CAV-1, the additional CAV-1 protein was distributed more towards the plasma membrane compared to the CAV-1 constitutively expressed in normal A7r5 cells (compare Figs. 2 and 3). The increased partitioning of CAV-1 to the plasma membrane, along with the presumed increase in CAV-1 levels resulted in a marked redistribution of PFK and ALD in the cell towards the plasma membrane. Although there is some variation in the PFK signal in the cytoplasm of the CAV-1 over-expressing cells (see Fig. 3 and the intensity graphs in Fig. 4b), the general trend clearly indicates a significant shift to the plasma membrane (see Fig. 5b). Assuming the human CAV-1 that is over-expressed has the same affinity for PFK and ALD as the CAV-1 endogenously expressed in

the rat cell line, the increased glycolytic enzyme targeting to the plasma membrane is likely due to increased CAV-1 partitioning to the plasma membrane. A further implication of these findings is that other putative PFK binding sites in the cytoplasm must bind PFK and ALD with an affinity similar to, or moderately lower than, CAV-1. If the cytoplasmic binding sites had a far greater binding affinity than CAV-1, then increasing CAV-1 levels would have little effect on the glycolytic enzyme distribution.

CAV-1 over-expressing cells exhibited a small but significant increase in the percentage of PFK that overlapped with CAV-1 (see Fig. 6). An increase in the percentage of PFK which overlaps with CAV-1 could be accomplished by (1) increasing the total number of CAV-1 molecules (which did occur, see Fig. 1); (2) increasing the affinity of CAV-1 molecules for PFK; or (3) by decreasing the number or affinity of competing binding sites for PFK. Since it is unlikely that the affinity of the over-expressed CAV-1 is different than the native CAV-1, the most likely explanation for our results is that an increase in the number of CAV-1 sites resulted in a higher percentage of PFK being bound to CAV-1.

Since localization of the entire series of glycolytic enzymes may be viewed as required to localize the entire flux to the membrane, we examined whether CAV-1 over-expression altered the localization of ALD to the same extent as it did PFK. The very clear overlap of PFK and ALD in both control and CAV-1 over-expressing cells suggests that either ALD also interacts with CAV-1, that ALD and PFK directly interact, or the proteins all colocalize due to common interaction with an accessory protein. In any of these cases, CAV-1 localization to the plasma membrane appears to be the critical event that results in localization of at least some glycolytic enzymes to the plasma membrane.

This study demonstrates that the localization of PFK and ALD within a smooth muscle cell depends on the relative distribution of scaffolding proteins for the binding of PFK, such that changes in the number of membrane binding sites change the membrane localization of the glycolytic enzymes. Presumably, altering the number or affinity of other binding sites (such as cytoskeletal actin or microtubules) would also result in a redistribution of this glycolytic enzyme. Therefore, glycolytic enzyme localization, and hence glycolytic ATP production may be dynamically redistributed within the cell according to the distribution of appropriate scaffolding proteins. The multiple compartments of glycolysis may thus be regulated by the number and affinity of glycolytic enzyme binding sites, many of which change with disease states and switches in cell phenotype.

REFERENCES

Anderson RG. 1998. The caveolae membrane system. Annu Rev Biochem 67:199–225.

Beitner R. 1993. Control of glycolytic enzymes through binding to cell structures and by glucose-1,6-bisphosphate under different conditions. The role of Ca^{2+} and calmodulin. Int J Biochem 25:297–305.

Campanella ME, Chu H, Low PS. 2005. Assembly and regulation of a glycolytic enzyme complex on the human erythrocyte membrane. Proc Natl Acad Sci USA 102: 2402–2407.

Campbell JD, Paul RJ. 1992. The nature of fuel provision for the Na^{+}-K^{+}-ATPase in vascular smooth muscle. J Physiol 447:67–82.

Clegg JS, Jackson SA. 1989. Evidence for intermediate channelling in the glycolytic pathway of permeabilized L-929 cells. Biochem Biophys Res Commun 160:1409–1414.

Goodwin GW, Ahmad F, Taegtmeyer H. 1996. Preferential oxidation of glycogen in isolated working rat heart. J Clin Invest 97:1409–1416.

Hardin CD, Finder DR. 1998. Glycolytic flux in permeabilized freshly isolated vascular smooth muscle cells. Am J Physiol Cell Physiol 43:88–96.

Hardin CD, Kushmerick MJ. 1994. Simultaneous and separable flux of pathways for glucose and glycogen utilization studied by ^{13}C-NMR. J Mol Cell Cardiol 26:1197–210.

Hardin CD, Paul RJ. 1992. Localization of two glycolytic enzymes in guinea-pig taenia coli. Biochim Biophys Acta 1134:256–259.

Hardin CD, Paul RJ. 1995. Metabolism and energetics of vascular smooth muscle. In: Sperelakis NS, editor. Physiology and pathophysiology of the heart. Boston: Kluwer Academic Publishers. pp 1069–1086.

Hardin CD, Roberts TM. 1995a. Compartmentation of glucose and fructose 1,6-bisphosphate metabolism in vascular smooth muscle. Biochemistry 34:1323–1331.

Hardin CD, Roberts TM. 1995b. Gluconeogenesis during hypoxia in vascular smooth muscle studied by ^{13}C-NMR. Physiol Res 44:257–260.

Hardin CD, Raeymaekers L, Paul RJ. 1992. Comparison of endogenous and exogenous sources of ATP in fueling Ca^{2+} uptake in smooth muscle plasma membrane vesicles. J Gen Physiol 99:21–40.

Jenkins JD, Madden DP, Steck TL. 1984. Association of phosphofructokinase and aldolase with the membrane of the intact erythrocyte. J Biol Chem 259:9374–9378.

Jenkins JD, Kezdy FJ, Steck TL. 1985. Mode of interaction of phosphofructokinase with the erythrocyte membrane. J Biol Chem 260:10426–10433.

Knull HR, Laursen SE, Cottick AA. 1987. Cytomatrix—glycolytic enzyme interactions: "Molecular Mechanisms in the Regulation of Cell Behavior." Liss, NY. pp 157–161.

Leach RM, Hill HM, Snetkov VA, Robertson TP, Ward JPT. 2001. Divergent roles of glycolysis and the mitochondrial electron transport chain in hypoxic pulmonary vasoconstriction of the rat: Identity of the hypoxic sensor. J Physiol 536:211–224.

Lehotzky A, Telegdi M, Liliom K, Ovadi J. 1993. Interaction of phosphofructokinase with tubulin and microtubules. Quantitative evaluation of the mutual effects. J Biol Chem 268:10888–10894.

Lloyd PG, Hardin CD. 1999. Role of microtubules in the regulation of metabolism in isolated cerebral microvessels. Am J Physiol 277:C1250–C1262.

Lloyd PG, Hardin CD. 2000. Sorting of metabolic pathway flux by the plasma membrane in cerebrovascular smooth muscle cells. Am J Physiol 278:C803–C811.

Lloyd PG, Hardin CD. 2001. Caveolae and the organization of carbohydrate metabolism in vascular smooth muscle. J Cell Biochem 82:399–408.

Low PS, Rathinavelu P, Harrison ML. 1993. Regulation of glycolysis via reversible enzyme binding to the membrane protein, band 3. J Biol Chem 268:14627–14631.

Luetterforst R, Stang E, Zorzi N, Carozzi A, Way M, Parton RG. 1999. Molecular characterization of caveolin association with the Golgi complex: Identification of a *cis*-Golgi targeting domain in the caveolin molecule. J Cell Biol 145:1443–1459.

Lynch RM, Paul RJ. 1983. Compartmentation of glycolytic and glycogenolytic metabolism in vascular smooth muscle. Science 222:1344–1346.

Lynch RM, Paul RJ. 1987. Compartmentation of carbohydrate metabolism in vascular smooth muscle. Am J Physiol 252:C328–C334.

Machleidt T, Li WP, Liu P, Anderson RG. 2000. Multiple domains in caveolin-1 control its intracellular traffic. J Cell Biol 148:17–28.

Ouporov IV, Knull HR, Thomasson KA. 1999. Brownian dynamics simulations of interactions between aldolase and G- or F-actin. Biophys J 76:17–27.

Ouporov IV, Keith TJ, Knull HR, Thomasson KA. 2000. Computer simulations of glycolytic enzyme interactions with F-actin. J Biomol Struct Dyn 18:311–323.

Pagliaro L, Taylor DL. 1988. Aldolase exists in both the fluid and solid phases of cytoplasm. J Cell Biol 107:981–991.

Pagliaro L, Taylor DL. 1992. 2-Deoxyglucose and cytochalasin D modulate aldolase mobility in living 3T3 cells. J Cell Biol 118:859–863.

Paul RJ. 1980. Chemical energetics of vascular smooth muscle: "Handbook of Physiology—The Cardiovascular System II." Bethesda, MD: American Physiological Society. pp 201–235.

Paul RJ, Hardin CD, Raeymaekers L, Wuytack F, Casteels R. 1989. Preferential support of Ca^{2+} uptake in smooth muscle plasma membrane vesicles by an endogenous glycolytic cascade. FASEB J 3:2298–2301.

Razani B, Woodman SE, Lisanti MP. 2002. Caveolae: From cell biology to animal physiology. Pharmacol Rev 54:431–467.

Scherer PE, Lisanti MP. 1997. Association of phosphofructokinase-M with caveolin-3 in differentiated skeletal myotubes. Dynamic regulation by extracellular glucose and intracellular metabolites. J Biol Chem 272:20698–20705.

Schlegel A, Lisanti MP. 2001. Caveolae and their coat proteins, the caveolins: From electron microscopic novelty to biological launching pad. J Cell Physiol 186:329–337.

Smart EJ, Graf GA, McNiven MA, Sessa WC, Engelman JA, Scherer PE, Okamoto T, Lisanti MP. 1999. Caveolins, liquid-ordered domains, and signal transduction. Mol Cell Biol 19:7289–7304.

Sotgia F, Bonuccelli G, Minetti C, Woodman SE, Capozza F, Kemp RG, Scherer PE, Lisanti MP. 2003. Phosphofructokinase muscle-specific isoform requires caveolin-3 expression for plasma membrane recruitment and caveolar targeting: Implications for the pathogenesis of caveolin-related muscle diseases. Am J Pathol 163:2619–2634.

Taggart MJ. 2001. Smooth muscle excitation-contraction coupling: A role for caveolae and caveolins? News in Physiol Sci 16:61–65.

Thyberg J. 2000. Differences in caveolae dynamics in vascular smooth muscle cells of different phenotypes. Lab Invest 80:915–929.

Vallejo J, Hardin CD. 2004a. Caveolin-1 functions as a scaffolding protein for phosphofructokinase in the metabolic organization of vascular smooth muscle. Biochemistry 43:16224–16232.

Vallejo J, Hardin CD. 2004b. Metabolic organization in vascular smooth muscle: Distribution and localization of caveolin-1 and phosphofructokinase. Am J Physiol Cell Physiol 286:C43–C54.

Vallejo J, Hardin CD. 2005. Expression of caveolin-1 in lymphocytes induces caveolae formation and recruitment of phosphofructokinase to the plasma membrane. FASEB J 19:586–587.

Vertessy BG, Kovacs J, Ovadi J. 1996. Specific characteristics of phosphofructokinase-microtubule interaction. FEBS Lett 379:191–195.

Volker KW, Knull HR. 1993. Glycolytic enzyme-tubulin interactions: Role of tubulin carboxy terminals. J Mol Recog 6:167–177.

Volker KW, Reinitz CA, Knull HR. 1995. Glycolytic enzymes and assembly of microtubule networks. Comp Biochem Physiol B Biochem Mol Biol 112:503–514.

von Ruckmann B, Schubert D. 2002. The complex of band 3 protein of the human erythrocyte membrane and glyceraldehyde-3-phosphate dehydrogenase: Stoichiometry and competition by aldolase. Biochim Biophys Acta 1559:43–55.